Spring 5-13-2013

Why Do Molecules Echo Atomic Periodicity?

Ray Hefferlin
Southern Adventist University, hefferln@southern.edu

Jonathan Sackett
Southern Adventist University, hefferln@southern.edu

Jeremy Tatum
University of Victoria, jtatum@uvic.ca

Recommended Citation
International Journal of Quantum Chemistry, 113, 2078-2089, 2013 (DOI10.1002/qua.24469)

International Journal of QUANTUM CHEMISTRY

Why Do Molecules Echo Atomic Periodicity?

Ray Hefferlin,*[a] Jonathan Sackett,[a] and Jeremy Tatum[b]

Franck–Condon factors are investigated for sequences of free main-group diatomic molecules. Theory-based Condon loci (parabolas) and Morse-potential loci are plotted on Deslandres tables to verify if they, indeed, follow the largest Franck–Condon factors. Then, the inclination angles of the Condon loci are determined. Thus, entire band systems are quantified by one variable, the angle. For all available isoelectronic sequences, this angle increases from a central minimum toward magic-number molecular boundaries. The theory for the Condon locus gives the angle in terms of the ratio of the upper-state to the lower-state force constants. It is concluded that the periodicity is caused due to the fact that this ratio becomes larger as rare-gas molecules are approached, a trend that probably points to the extreme cases of the rare-gas molecules themselves. Thus, molecular periodicity echoes atomic periodicity in that data plots have extrema at molecules with magic-number atoms, yet it does not echo the details of atomic periodicity in series between those molecules. © 2013 The Authors. International Journal of Quantum Chemistry Published by Wiley Periodicals, Inc.

DOI: 10.1002/qua.24469

Introduction

An understanding of molecular periodicity that has a basis in quantum states is highly desired, so this article reports the behaviors of the force constants of the upper and lower states of many band systems for which spectroscopic constants and Franck–Condon factor (FCF) tables are known. The ratio of the two force constants determines the periodic behavior.

Molecules do echo atomic periodicity, because data for series of molecules are repetitious with periods bounded by molecules having atomic numbers Z_A and Z_B (or both) equal to an atomic magic number—even from one pair of periods to another. Several properties of diatomic molecules AB display this limited kind of periodic behavior when plotted with regard to their atomic-number coordinates Z_A and Z_B. They include internuclear separations r_e,[1] vibration frequencies ω_e,[1] and *ab initio* force constants k,[2] but all just for ground states, and ionization potentials.[1] Entire Deslandres tables of band-system FCFs have recently been studied along many isoelectronic sequences.[3] In this work, the spring constants of both the upper and lower states play a role.

The periodicities just described do not echo atomic periodicity in detail; there are rare similarities between graphs of properties with changing Z_A and fixed Z_B on the one hand and graphs of the same properties for atoms with changing Z_A on the other—even for neutral, gas-phase, main-group species. Cases where a similarity does exist are related to additivity, for instance, various radiation cross-sections in the high-energy limit and internuclear separations that are approximately equal to the sum of their covalent radii of atoms. A more generally applicable rationale than additivity, as to why any periodicity at all exists, is badly needed. Such a rationale should also apply to properties for which no atomic analog exists.

The periodic behavior of the vibration frequencies ω_e'' of ground-state main-group diatomic molecules has been reported before.[1] It remains in this article to consider the behavior of ω_e' and thence of k'/k''. This is done by the use of Condon loci, which have been assumed to follow the tracks of maximally high FCFs.

The exploration shows that the cause of periodicity is that the upper level force constant becomes stronger and stronger, compared to the lower level force constant, as a noble-gas molecule is approached. Thus, the two eigenstates are responsible for the observed periodicity.

Theory

"Simple-harmonic motion" (SHM) electronic potentials

The locally maximum FCFs in a Deslandres table can be connected like dots in a child's puzzle. The result is a curve called the Condon locus, which more[4] or less[5–7] resembles a parabola (Fig. 1).

Classically, it is clear that the most likely transitions are at internuclear separations at the extrema of the motion, when one upper-state extremum is directly above a lower-state extremum (Fig. 2). The FCF for that band will be large compared to others, and the totality of all such factors is the Condon locus. Quantum mechanically the strongest transitions will occur when the wave function antinodes are more or less one above the other near the classical extrema. The wave functions also allow relatively strong transitions when the antinodes are above one another but not at the

[a] *R. Hefferlin, J. Sackett*
Department of Physics, Southern Adventist University, Post Office Box 307, Collegedale, Tennessee, 37315
E-mail: hefferln@southern.edu
[b] *J. Tatum*
Department of Astronomy, University of Victoria, Victoria, British Columbia V8W 2Y2, Canada

Contract grant sponsor: Donors to Southern Adventist University.

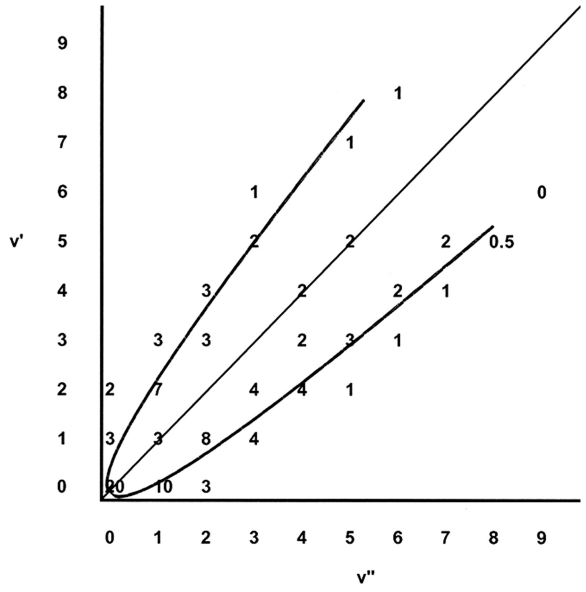

Figure 1. A Deslandres table showing some locally maximal FCFs $q(v',v'')$. The simple harmonic approximation Condon locus is shown. The locus symmetry axis appears to lie at 45° from v''. Adapted from Herzberg,[4] pg. 197.

classical extrema; such transitions will form secondary Condon loci.[5–7]

The transitions that occur when the molecule is at an internuclear separation matching the end-points of vibrational states, in both the upper and lower electronic levels, will have the highest FCFs. The probability of finding the molecule at a given internuclear separation is shown schematically in Figure 2 for the upper state. These transitions take place almost instantaneously, in a time that is very short compared with the period of molecular vibration (the Born–Oppenheimer approximation); they take place with virtually no change in internuclear distance. For that reason, transitions can be indicated in energy level diagrams by means of vertical lines.

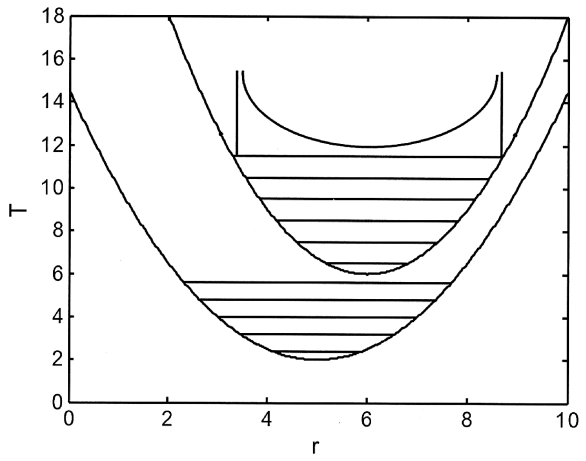

Figure 2. Schematic of two SHM potential-energy curves of a molecule, with energy on the vertical axis and internuclear separation on the horizontal axis. The uppermost feature represents the probability of finding a classical oscillator at points in its domain.

If we take it as given that the two electronic potentials are parabolas, it is a good exercise in conic sections to show that the Condon locus that follows the strongest FCFs is also a parabola. The derivation appears in full in Ref. 3]; here, we review the results. The slope of the axis of the Condon parabola with respect to v'' is given simply by

$$\tan\theta = \frac{\omega'_e}{\omega''_e} \tag{1}$$

or

$$\tan\theta = \sqrt{\frac{k'}{k''}}, \tag{2}$$

where ω_e are in cm^{-1}, the k are force constants, and the single and double primes indicate the upper and lower electronic potentials. The length of the latus rectum is given by

$$2l = \frac{4\left(r''_e - r'_e\right)^2 \omega''_e{}^2 \omega'_e{}^2}{L\left(\omega''_e{}^2 + \omega'_e{}^2\right)^{3/2}}, \tag{3}$$

with l being dimensionless and L having units of cm, and where

$$L = \frac{\hbar}{\pi mc}. \tag{4}$$

The latera recta are taken to have the same length scale as the quantum numbers v' and v and m is the reduced mass. The behaviors of the lower-state vibration frequencies are well-studied and smooth[1]; those of the upper-state vibration frequencies are irregular, and these irregularities account for the deviations of data point in the graphs to be shown in a later section.

The derivation implies the following:

1. If $\theta = 45°$, then the force constants in the two potentials are equal. If θ is smaller, then the lower electronic state is more tightly bound than the upper state.
2. A Condon parabola has its vertical and horizontal tangents at $v = -1/2$.
3. If the internuclear distances are equal, the parabola degenerates to a straight line, and the strongest bands have coordinates $(v',v'') = (0,0)$, (1,1), (2,2), and so on. Otherwise, the parabola is open.

Morse and other anharmonic potential curves

The Condon loci for Morse potentials can be calculated in much the same way as the simple harmonic case, except that additional anharmonic spectroscopic constants are necessary. The same applies also to all anharmonic potentials, such as the Lennard–Jones potential or indeed any potential function, even if the potential is given only as a table of numerical values.

Table 1. Diatomic molecules in this study, sorted according to qualitative appearance of loci and then the latus rectum.

Species	Band system	(C1,C2)	Theta degrees	Latus rectum
1 SHM and Morse loci nearly identical				
MgF	B-X	(2,7)	46.54	0.1611
2 Morse locus arms above SHM arms				
MgF	A-X	(2,7)	46.24	0.0016
C_2	D-X	(4,4)	44.61	0.0048
AlF	A-X	(3,7)	45.06	0.0065
CO	C-X	(4,6)	44.24	0.0229
BeBr	A-X	(2,7)	44.33	0.0634
BeF	B-X	(2,7)	47.28	0.112
BeF	A-X	(2,7)	42.79	0.1618
BeO	B-X	(2,6)	42.67	0.1694
LuF	D-X	(3,7)[a]	42.96	0.2018
CS[b]	a-X	(4,6)	31.45	0.2394
PO[b]	B-A	(5,6)	39.94	0.2834
CS	A-X	(4,6)	39.87	0.3191
BF	A-X	(3,7)	43.36	0.4115
AlO	B-X	(3,6)	41.62	0.4638
PN	A-X	(5,5)	39.52	0.7449
SiN	A-X	(4,5)	42.21	0.8674
CN	A-X	(4,5)	41.22	0.9797
C_2	A-X	(4,4)	40.93	1.2332
MgO	A′-X	(2,6)	40.24	1.3398
Li_2	B-X	(1,1)	37.44	1.4793
CO	a-X	(4,6)	38.78	1.6168
CP	A-X	(4,5)	40.59	1.6856
BO	B-X	(3,6)	34.25	1.9408
SiO	A-X	(4,6)	34.48	2.4094
SnO	D-X	(4,6)	35.15	2.4953
BeO	A-X	(2,6)	37.57	2.6193
CP	B-X	(4,5)	34.00	2.6683
CO	A-X	(4,6)	34.98	2.7208
SiS	D-X	(4,6)	34.39	2.9384
K_2	B-X	(1,1)	39.18	3.099
Li_2	C-X	(1,1)	34.10	3.1077
BeS	A-X	(2,6)	37.38	3.3577
N_2	B-X	(5,5)	36.31	3.6556
Na_2	B-X	(1,1)	37.98	3.8289
AlO	A-X	(3,6)	36.65	3.8982
CSe	A-X	(4,6)	38.3	4.0352
BO	A-X	(3,6)	33.77	4.1475
BS	E-X	(3,6)	33.12	5.5527
BS	A-X	(3,6)	32.53	6.1045
3 Morse locus arms below SHM arms				
SiN	B-X	(4,5)	41.84	0.0132
BeCl	A-X	(2,7)	44.16	0.0722
BeCl	B-X	(2,7)	48.37	0.4026
SN	C-B′	(4,5)	52.65	0.4463
BF	B-X	(2,7)	50.38	0.6681
SiF	C′-X	(4,7)	50.28	1.1434
F_2	F-X	(7,7)	51.03	2.373
4 Morse lower arm falls to lower right				
SiF	B-A	(4,7)	54.60	0.75
5 Morse curls up from SHM locus				
CaH	B-X	(2,1)	44.70	0.0197
CaH	A-X	(2,1)	45.75	0.0207
MgH	A-X	(2,1)	46.91	0.081
6 Morse arms inside and cross or will cross				
AlF	b-X	(3,7)	44.43	0.0433
BCl	A-X	(3,7)	45.34	0.1002
CN	B-X	(4,5)	46.29	0.1361
BF	b-X	(3,7)	49.29	0.4941
7 Morse arms outside of SHM arms				
PO	A-B	(5,6)	50.05	0.2833
8 Resemblance to theater curtains				
K_2	C-X	(1,1)	33.75	7.605
ICl	B-X	(7,7)	28.92	17.644
Cl_2	B-X	(7,7)	24.87	18.7019
BrCl	B-X	(7,7)	26.62	18.8425
NaK	C-X	(1,1)	29.88	19.2268
IBr	B-X	(7,7)	27.86	19.5107
Br2	B-X	(7,7)	27.26	22.3234
I_2	B-X	(7,7)	30.37	22.8193
9 Symmetry axes appear to cross				
LiH	B-X	(1,1)	9.62	0.9345
NaH	A-X	(1,1)	14.84	7.4362
10 Loci resemble part of a wheel				
SiO	a-X	(4,6)	32.47	6.5969
IF	B-X	(7,7)	33.98	6.7172
SN	B-X	(6,5)	33.22	7.2826
N_2	a′-X	(5,5)	32.98	7.6974
N_2	A-X	(5,5)	31.77	8.2393
ClF	B-X	(7,7)	18.50	8.8923
CO	a′-X	(4,6)	29.52	9.3526
CaO	A′-X	(2,6)	36.70	10.4253
PO	B′-X	(5,6)	31.62	10.5156
SrO	A′-X	(2,6)	35.89	11.7849

Not all of these molecules are known to have published Franck–Condon factors. Some of those that do have FCFs have been studied exhaustively and are featured in the next section.

[a]The group number of Lu is chosen as 3 (in main group elements with groups 1 to 8).

[b]The upper arm of the Morse locus rises high above that the SHM upper arm.

The derivation which follows is classical, based on the premise that, at any instant of time, the molecule is most likely to be at its vibrational energy level position of greatest compression or greatest separation. For a quantum mechanical calculation, one can assume that, at any instant of time, the internuclear separation is most likely to be in both levels where there are maximum antinodes of the wave function. For large values of the vibrational quantum number, these maxima are close to the classical extrema; the classical approximation will become less accurate at very low quantum numbers.

Suppose that the potential energy functions of the two electronic states are

$$V' = V'_e + D'_e\left[1-\exp\left(-\frac{(r-r'_e)}{a'}\right)\right]^2,$$
$$V'' = V''_e + D''_e\left[1-\exp\left(-\frac{(r-r''_e)}{a''}\right)\right]^2. \quad (5)$$

Both D_e are the depths of the potential wells. V_e' and V_e'' do not come into the calculation of the FCFs, so we might as well take both of them to be zero. Thus, the potential functions are

$$V' = D'_e\left[1-\exp\left(-\frac{(r-r'_e)}{a'}\right)\right]^2,$$
$$V'' = D''_e\left[1-\exp\left(-\frac{(r-r''_e)}{a''}\right)\right]^2. \quad (6)$$

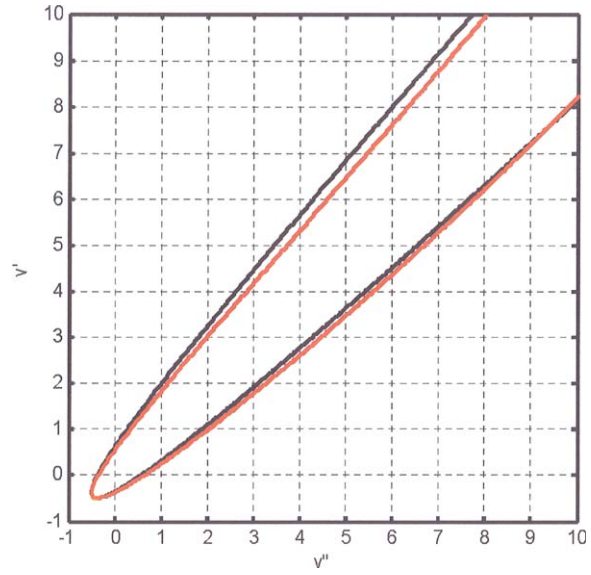

Figure 3. The SHM and Morse loci for the MgF $B^2\Sigma^+$-$X^2\Sigma^+$ band system in the $q(v',v'')$ plane where each axis goes from −1 to 10. This system is the only known entry in Class 1, where the two loci coincide very well in this limited domain. [Color figure can be viewed in the online issue, which is available at wileyonlinelibrary.com.]

The a' and a'' are given in terms of the spectroscopic constants by

$$a=\sqrt{\frac{\hbar}{4\pi mc\omega_e x_e}}=4.105805\times10^{-9}/\sqrt{m\omega_e x_e}m. \qquad (7)$$

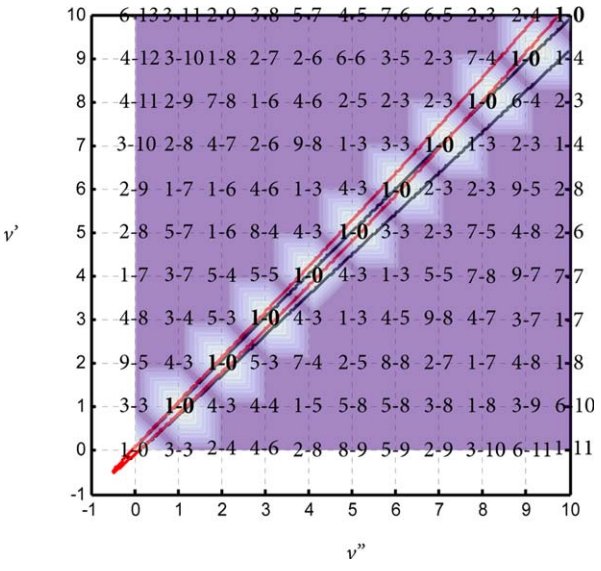

Figure 4. The $q(v',v'')$ space is displayed as a terrain with locally maximal FCFs in bold face. Entries such as 7-4 represent values in the form 7×10^{-4}. The SHM and Morse loci for the C2 $D^1\Sigma_u^+$-$X^1\Sigma_g^+$ band system (Class 2) are in black and red, respectively; they are similar except that the latter is tilted somewhat above the former. The latus rectum is extremely small, indicating that the electronic potentials have very similar internuclear separations. The symmetry axis of the SHM locus (θ) is 44.61°, which coincides with the angle of the bold face FCFs (seemingly 45°) extremely well. The θ value indicates that the vibration frequencies and force constants of the upper and lower electronic states are very similar. [Color figure can be viewed in the online issue, which is available at wileyonlinelibrary.com.]

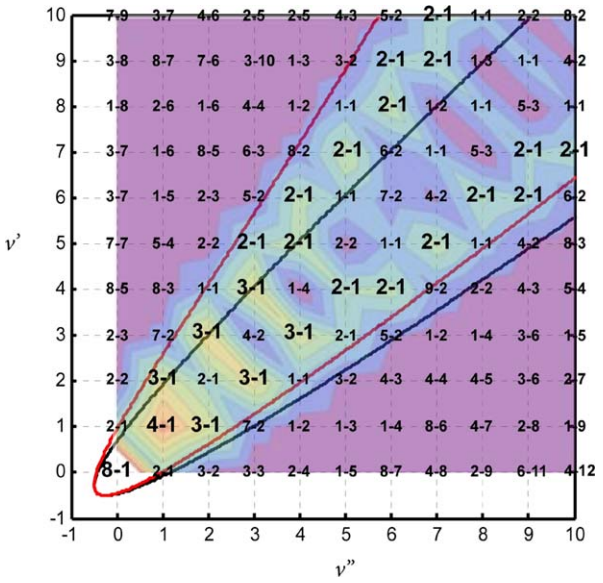

Figure 5. The SHM and Morse loci for the CS $a^3\Pi_r$-$X^1\Sigma^+$ band system of Class 2. The upper arm of the SHM locus follows the local maxima for a while and then drops below; the lower arm is always below. Both arms of the Morse locus are above the two arms of the SHM locus; the lower one by a small amount, which brings it closer to the local maxima, and the upper arm by a very large amount. The SHM locus is about the same shape as the track suggested by the contours but lies at a smaller angle. Its angle θ is 41.45°, indicating that the internuclear separations are not as similar as in Figure 4. The slope of the locally maximal FCFs is about 45°, so the two slopes differ by less than 5°. [Color figure can be viewed in the online issue, which is available at wileyonlinelibrary.com.]

The $\omega_e x_e$ is the anharmonicity constant in m^{-1} and m is the reduced mass in amu. D_e' and $D_e''$are given in terms of the spectroscopic constants by

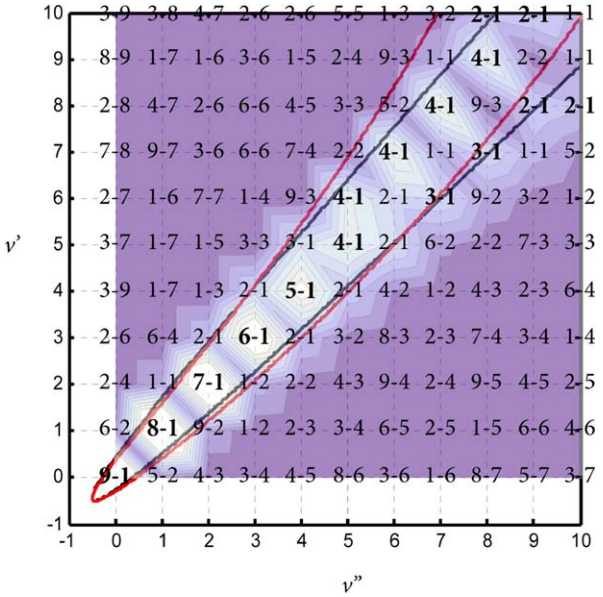

Figure 6. The SHM and Morse loci for MgH $A^2\Pi_r$-$X^2\Sigma^+$ (Class 5) showing how they are similar for small values of v' and v'' and how the Morse locus curves up and away at larger vibrational quantum numbers. The θ for the SHM locus is 46.91°, which agrees well with the 45° slope of the bifurcated bold-face local maximum track and indicates not so dissimilar internuclear separations. [Color figure can be viewed in the online issue, which is available at wileyonlinelibrary.com.]

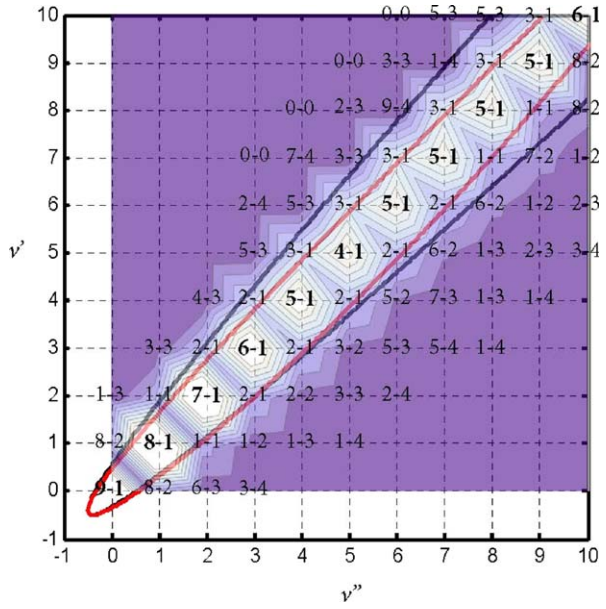

Figure 7. The SHM and Morse loci for CN $B^2\Sigma^+$-$X^2\Sigma^+$. The "average" of the two inner branches of the Morse locus starts with a slightly lower angle from the v'' axis than does the symmetry axis of the SHM locus; then this "average" turns with very slight upward curvature (point 3 in the section Theory). At the same time, the inner curves appear to converge (point 4). The SHM latus rectum is rather small, indicating that the electronic potentials have somewhat similar internuclear separations. The angle θ is 46.29°, in good agreement with the 45° symmetry angle of the bold-face local maxima. [Color figure can be viewed in the online issue, which is available at wileyonlinelibrary.com.]

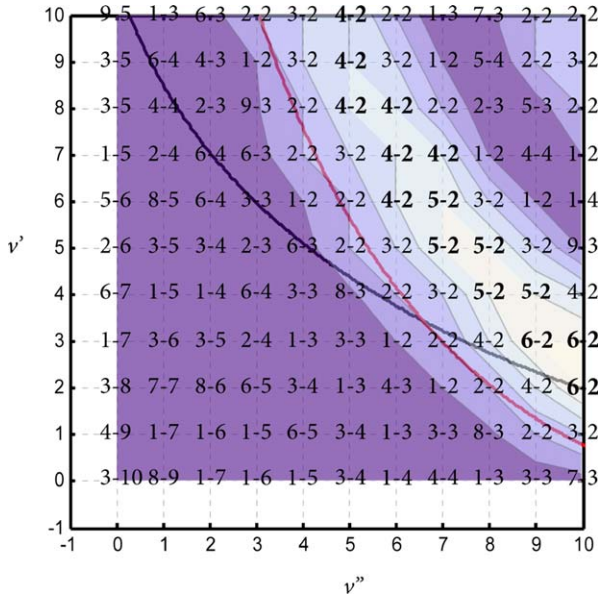

Figure 8. The $B^3\Pi_u$-$X^1\Sigma_g^+$, one of two parts of the $B^3\Pi_u(O_u^+)$-$X^1\Sigma_g$ band system of Br2. This appearance was called "theater curtains" in Table 1. The Morse locus seems to follow the local maxima rather well but is displaced at about 1.5 units toward the origin. The SHM locus seems at first glance to have a different symmetry-axis angle (27.26°) than does the track of local maximal FCFs. A graphic extending to quantum numbers 40 (not shown) demonstrates, however, that the symmetry angle of the FCFs is indeed close to 27°, indicating that the force constants for the upper electronic state are much less than for the lower state. Secondary Condon loci, of which there have been hints in the previous figures, are clearly visible in the raw data. [Color figure can be viewed in the online issue, which is available at wileyonlinelibrary.com.]

$$D_e = \frac{\omega_e^2 hc}{4\omega_e x_e}. \tag{8}$$

One begins by taking some value of V' (between 0 and D_e') and we calculate the extreme values of r, which we call r_L and r_R (for left and right). These are given by

$$r_L = r'_e - a' \ln\left(1 + \sqrt{\frac{V'}{D'_e}}\right),$$
$$r_R = r'_e - a' \ln\left(1 - \sqrt{\frac{V'}{D'_e}}\right). \tag{9}$$

Now, one goes to the lower potential curve and to eq. (6b). One chooses $r = r_L$ and $r = r_R$ to find the two corresponding values of V''. This process gives two points of the Condon locus in the (V', V'') plane.

To go from the (V',V'') plane to the (v',v'') plane, one uses

$$V'/(hc) = \left(v' + \frac{1}{2}\right)\omega'_e - \left(v' + \frac{1}{2}\right)^2 \omega'_e x'_e$$
$$V''/(hc) = \left(v'' + \frac{1}{2}\right)\omega''_e - \left(v'' + \frac{1}{2}\right)^2 \omega''_e x''_e. \tag{10}$$

One inverts these quadratic formulae in $(v + 1/2)$, eq. (10), to obtain

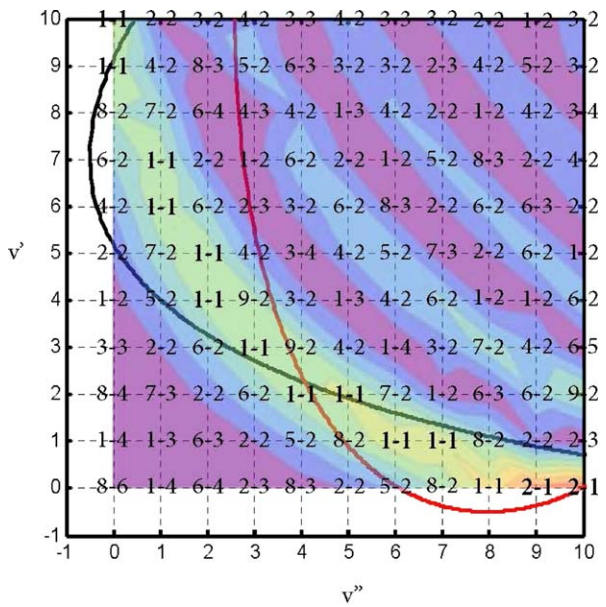

Figure 9. The NaH $A^1\Sigma^+$-$X^1\Sigma^+$ FCFs and loci. Even in this limited v' and v'' domain, it is clear that the SHM locus does not follow the local maxima. The SHM locus has an inclination of 14.84°, indicating that the upper state is much less tightly bound than the ground state. The latus rectum is very large, indicating very different internuclear separations on the two electronic states. Secondary Condon loci are clearly visible in the raw data. The symmetry angle of the bold-face number track(s) is impossible to ascertain. [Color figure can be viewed in the online issue, which is available at wileyonlinelibrary.com.]

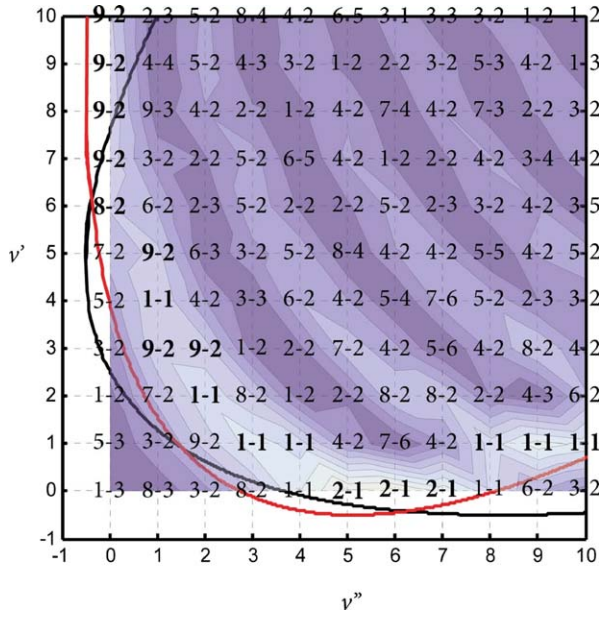

Figure 10. The N2 $A^3\Sigma_u^+$-$X^1\Sigma_g^+$ FCFs and loci. The SHM locus has an inclination of 31.77°, indicating that the triplet upper state has a smaller force constant than the singlet ground state. The appearance of this graphic was described in Table 1 as resembling part of a wheel.

$$v' = \frac{\omega'_e - \sqrt{\omega'^2_e - 4\omega'_e x'_e V'/(hc)}}{2\omega'_e x'_e} - \frac{1}{2}$$
$$v'' = \frac{\omega''_e - \sqrt{\omega''^2_e - 4\omega''_e x''_e V''/(hc)}}{2\omega''_e x''_e} - \frac{1}{2}. \quad (11)$$

Thus, one has two points of the Condon locus in the (v', v'') plane, one on each branch of the locus. Repeat for many values of V_e' between 0 and D_e' to delineate the Condon locus. Note that $v = \omega_e/(2\omega_e x_e)$ corresponds to a vibrational level whose energy is equal to the dissociation limit. In principle, vibrational levels with larger values of v (with energies below the dissociation limit), and transitions from them, are possible. These are unlikely to be observed, and so we restrict our attention to solutions with a negative sign before the square roots in eqs. (11).

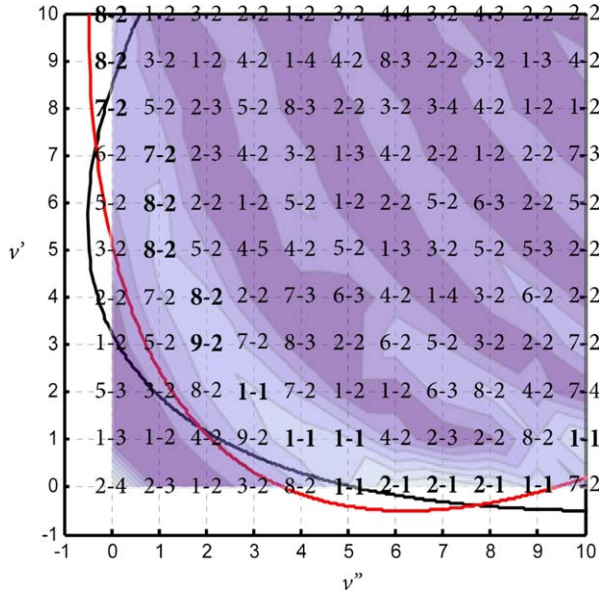

Figure 11. The band system CO $a'^3\Sigma^+$-$X^1\Sigma^+$ showing FCFs and loci very similar to those in Figure 10. The SHM locus has an inclination of 29.52°. [Color figure can be viewed in the online issue, which is available at wileyonlinelibrary.com.]

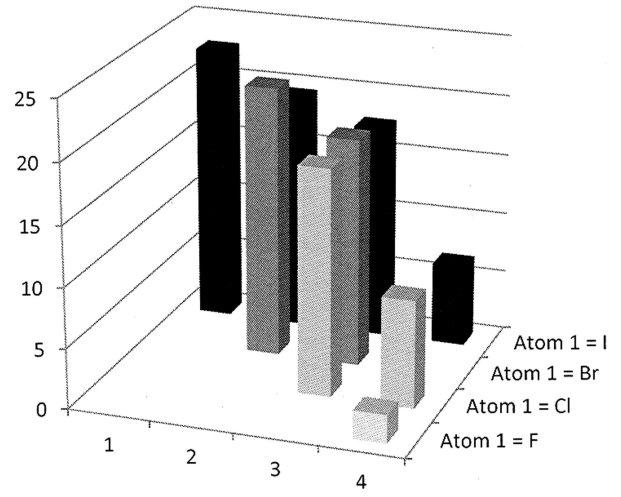

Figure 12. Latera recta plotted against R1 and R2 for the dihalides (C_1,C_2) = (7,7). The left to right numbers represent atom 2 as iodine, bromine, chlorine, and fluorine. The band systems are from Classes 3, 8, and 10 of Table 1.

The derivation, and computer experiments that were done afterward, imply the following:

1. The upper branch of the Condon locus will pertain to the horizontally asymptotic portion of the Morse curve of the upper electronic potential curve. (At a given instant of time, the molecule is more likely to be at its condition of greatest extension than of greatest compression.)
2. If the anharmonicity constants for the two electronic states are equal but not very large, there is little effect on the Condon locus.
3. If the anharmonicity constants are equal but very large, however, the Morse locus deviates with upward curvature from the SHM locus.
4. If the anharmonicity constants are unequal, with $\omega_e x_e' > \omega_e x_e''$, the Morse locus is inside the SHM locus and crosses itself.
5. If the anharmonicity constants are unequal, with $\omega_e x_e' < \omega_e x_e''$, then both arms of the Morse locus diverge outward from SHM locus.

Data

We computed Condon loci for SHM and Morse potentials for the 77 band systems that are listed in Table 1. The spectroscopic constants were taken from Refs. [8 and 9]. The entries are sorted according to qualitative appearance classes and within classes according to increasing latus rectum. (Somewhat ambiguous appearance descriptions will be clarified later.) The column with heading (C_1,C_2) gives the group numbers of the atoms in the same order as they appear in the names of

Table 2. Total electron count of molecules in the isoelectronic sequences, member molecules, band systems, atomic number difference, spectroscopic constants, latus rectum (in units of v' and v''), and the Condon locus symmetry angle from v'' (in degrees).

n_e	Species	System	Z_1-Z_2	ω_e'(cm^{-1})	r_e'(Å)	ω_e''(cm^{-1})	r_e''(Å)	Mass (amu)	Latus rectum	Angle (°)
23	AlNe		3							
	SiF	$C'^2\Pi$-$X^2\Pi_r$	5	1031.8	1.529	857.19	1.601	11.315	1.143	50.28
	PO	$B'^2\Pi$-$X^2\Pi_r$	7	759.238	1.717	1233.34	1.476	10.550	10.516	31.62
	SN	$B^2\Pi_r$-$X^2\Pi_r$	9[a]	798.053	1.697	1218.7	1.494	9.738	7.283	33.22
	ClC	Π-$X^2\Pi$	11[a]	–	–	866.10	1.645	8.934	–	–
	ArB		13							
23	AlNe		3							
	SiF	$B^2\Sigma^+$-$A^2\Sigma^+$	5	1011.23	1.541	718.5	1.605	11.314	0.75	54.6
	PO	$A^2\Sigma^+$-$B^2\Sigma^+$	7	1309.94	1.431	1164.51	1.463	10.548	0.283	50.05
	SN	$C^2\Sigma^+$-$B'^2\Sigma^+$	9	1389	1.446	1060	1.49	9.738	0.446	52.65
	ClC		11[b]							
	ArB		13							
22	MgNe		2							
	AlF	$A^1\Pi_i$-$X^1\Sigma^+$	4	803.94	1.648	802.26	1.654	11.146	0.006	45.06
	SiO	$A^1\Pi_i$-$X^1\Sigma^+$	6	852.8	1.621	1241.6	1.510	10.177	2.409	34.48
	PN	$A^1\Pi_i$-$X^1\Sigma^+$	8	1103.09	1.547	1337.2	1.491	9.6434	0.745	39.52
	SC	$A^1\Pi_i$-$X^1\Sigma^+$	10	1073.4	1.574	1285.1	1.535	8.7252	0.319	39.87
	ClB	$A^1\Pi_i$-$X^1\Sigma^+$	12	849.04	1.689	839.12	1.715	8.3732	0.100	45.34
	ArBe		14							
22	MgNe		2							
	AlF	$b^3\Sigma^+$-$X^1\Sigma^+$	4[b]	786.37	1.639	802.26	1.654	11.148	0.043	44.43
	SiO	$a^3\Sigma^+$-$X^1\Sigma^+$	6[b]	790	1.7	1241.557	1.510	10.177	6.510	32.47
	PN		8							
	SC	$a'^3\Sigma^+$-$X^1\Sigma^+$	10[b]	830.7	1.726	1285.08	1.535	8.725	0.239	31.45
	ClB		12							
	ArBe		14							
21	NeNa		15							
	FMg	$A^2\Pi_r$-$X^2\Sigma^+$	3[a]	743.06	1.7469	711.69	1.75	10.610	0.002	46.24
	OAl	$A^2\Pi_r$-$X^2\Sigma^+$	5[a]	728.5	1.7708	979.23	1.6179	10.042	3.896	36.65
	NSi	$A^2\Pi$r-$X^2\Sigma^+$	7	1044.41	1.6357	1151.4	1.5719	9.332	0.867	42.21
	CP	$A^2\Pi_r$-$X^2\Sigma^+$	9	1061.99	1.653	1239.7	1.5622	8.649	1.686	40.59
	BS	$A^2\Pi_r$-$X^2\Sigma^+$	11[a]	752.61	1.8182	1180.2	1.6092	8.189	6.104	32.53
	BeCl	$A^2\Pi_r$-$X^2\Sigma^+$	13[a]	822.11	1.8211	846.7	1.7971	7.166	0.072	44.16
	LiAr		15							
21	NeNa		1							
	FMg	$B^2\Sigma^+$-$X^2\Sigma^+$	3[a]	750.94	1.718	711.69	1.75	10.610	0.161	46.54
	OAl	$B^2\Sigma^+$-$X^2\Sigma^+$	5[a]	870.05	1.667	979.23	1.6179	10.042	0.464	41.62
	NSi	$B^2\Sigma^+$-$X^2\Sigma^+$	7	1031.03	1.580	1151.36	1.5719	9.332	0.013	41.84
	CP	$B^2\Sigma^+$-$X^2\Sigma^+$	9	836.32	1.689	1239.67	1.5622	8.650	2.668	34
	BS	$B^2\Sigma^+$-$X^2\Sigma^+$	11[a]	770	1.806	1180.17	1.6092	8.189	5.553	33.12
	BeCl	$B^2\Sigma^+$-$X^2\Sigma^+$	13[a]	952.5	1.742	846.7	1.7971	7.165	0.403	48.37
	LiAr		15							
14	BeNe									
	BF	$B^1\Sigma^+$-$X^1\Sigma^+$	−4[b]	1693.51	1.207	1402.13	1.263	6.970	0.698	50.38
	CO	$C^1\Sigma^+$-$X^1\Sigma^+$	−2[b]	2112.7	1.120	2169.814	1.128	6.856	0.0230	44.24
	N_2	$a'^1\Sigma^-_u$-$X^1\Sigma^+_g$	0[b]	1530.254	1.276	2358.57	1.100	7.001	7.697	32.98
	CO	$C^1\Sigma^+$-$X^1\Sigma^+$	2[b]	2112.7	1.120	2169.814	1.128	6.856	0.0230	44.24
	BF	$B^1\Sigma^+$-$X^1\Sigma^+$	4[b]	1693.51	1.207	1402.13	1.263	6.970	0.698	50.38
	BeNe									
14	BeNe									
	BF	$b^3\Sigma^+$-$X^1\Sigma^+$	−4[b]	1629.28	1.215	1402.13	1.263	6.970	0.494	49.29
	CO	$a'^3\Sigma^+$-$X^1\Sigma^+$	−2[b]	1228.6	1.352	2169.814	1.128	6.856	9.3530	29.52
	N_2	$A^3\Sigma^-_u$-$X^1\Sigma^+_g$	0[b]	1460.64	1.287	2358.57	1.100	7.001	8.239	31.73
	CO	$a'^3\Sigma^+$-$X^1\Sigma^+$	2[b]	1228.6	1.352	2169.814	1.128	6.856	9.353	29.52
	BF	$b^3\Sigma^+$-$X^1\Sigma^+$	4[b]	1629.28	1.215	1402.13	1.263	6.970	0.494	49.29
	BeNe									
13	CN		−1							
	NC	$B^2\Sigma^+$-$X^2\Sigma^+$	1	2163.9	1.150	2068.59	1.172	6.462	0.136	42.29
	OB	$B^2\Sigma^+$-$X^2\Sigma^+$	3	1281.69	1.305	1885.69	1.204	6.521	0.112	34.2
	FBe	$B^2\Sigma^+$-$X^2\Sigma^+$	5[a]	1350.8	1.335	1247.36	1.361	6.113	1.941	47.28
	NeLi		7							
13	CN		−1							
	NC	$A^2\Pi_i$-$X^2\Sigma^+$	1	1812.5	1.233	2068.59	1.172	6.462	1.000	41.22
	OB	$A^2\Pi_i$-$X^2\Sigma^+$	3	1260.7	1.353	1885.69	1.204	6.521	4.148	33.77

Table 2. *(Continued)*

n_e	Species	System	Z_1-Z_2	ω_e'(cm^{-1})	r_e'(Å)	ω_e''(cm^{-1})	r_e''(Å)	Mass (amu)	Latus rectum	Angle (°)
	FBe	$A^2\Pi_i$-$X^2\Sigma^+$	5[a]	1154.67	1	1247.36	1.361	6.113	0.162	42.79
	NeLi		7							
13	CN		−1							
	NC	$A^2\Pi_i$-$X^2\Sigma^+$	1	1812.5	1.233	2068.59	1.172	6.462	1.000	41.22
	SB	$A^2\Pi_i$-$X^2\Sigma^+$	3	753.61	1.8182	1180.17	1.609	8.189	6.113	32.56
	BrBe	$A^2\Pi_i$-$X^2\Sigma^+$	5[c]	698.5	1.976	715	1.953	8.089	0.063	44.33
	KrLi		7							

The last 13-electron section includes isoelectronic molecules with progressively increasing period number as a computer experiment. A previous version of this table appears as Table 1 in Quantum Systems in Chemistry and Physics, Progress in Theoretical Chemistry and Physics, Vol. 26 (2012), "Systematics and Prediction of Franck–Condon Factors," by R. Hefferlin, J. Sackett, and J. Tatum, Ch. 8, pp. 186–188.

[a]Uncertainties are indicated for one or more data in the critical tables. [No Π excited state is listed for CCl in Ref. 8]; the ground state entries are for use later on.

[b]The ground state data are an average of data for $X^2\Pi_{1/2}$ and $X^2\Pi_{3/2}$.

[c]No Σ excited state is listed and so no entries are given for either state in the second part of the table.

[d]The multiplicity or parity change is anomalous.[bDubious upper state assignment(s).

[f]Average of two very close data.

the molecules; the numbers go from 1 to 7. In Table 8.1 of Ref. [3], many of these same entries appear as members of isoelectronic sequences.

The latera recta go from 0.0018 to 22.82. The angles θ range from 9.62 to 54.6°; θ has significance that will be featured in the section Trends in Data for Fixed (C_1,C_2) Molecules. It is difficult to classify the members within these classes chemically. For instance, Class 8 includes six dihalides—but there are dihalides in Classes 3 and 10. Class 9 consists of alkali-metal pairs—but there are also such molecules in Classes 2 and 8.

Testing the Faithfulness of the Loci to Their FCFs

It is crucial to test how well the SHM and/or Morse loci correspond to the FCFs in the Deslandres tables. We will do this with a sample set of graphs showing the calculated loci superposed (in all but Fig. 3) on data in the tables. This test is crucial in substantiating a previous study of the periodicity of band-system Deslandres tables.[3]

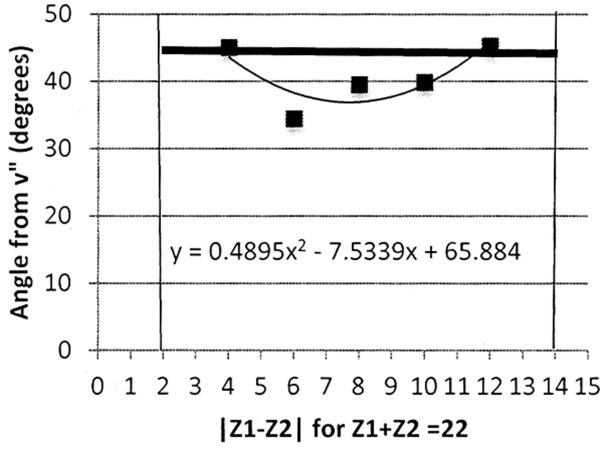

Figure 13. The angle θ of the loci for the 22-electron $^1\Pi_i$-$^1\Sigma^+$ portion of Table 2. The molecules AlF, SiO, PN, SC, and ClB have excited A states that are the second, seventh (it is the fifth, if one counts the triplet b state as one state), fifth, and second states above the ground state. The Condon loci for AlF and ClB are narrow; for the center three molecules, the loci are wide. The light vertical lines mark the positions of the rare-gas molecules MgNe and ArBe. The vertex is at $Z_1 - Z_2 = 7.696$, very close to half-way between these vertical lines.

There is only one molecule in Class 1, and Figure 3 makes it clear how well the loci coincide out to v' and $v'' = 10$. No FCF data are known, so the figure can not show how well the two loci agree with the data.

There are 40 entries in Class 2 (over half of the entries in the table); for these molecules, both the branches of the Morse locus are above those of the SHM locus. Two examples of this class are shown in Figures 4 and 5.

Class 3 molecules have the opposite appearance: The arms of the Morse locus are below those of the SHM locus. An extreme band system is that of SiF $B^2\Sigma^+$-$A^2\Sigma^+$ (Class 4), not shown, where the lower Morse arm is considerably below the lower SHM arm. Class 5 molecules have Morse loci curving upward, thus illustrating point 3, about very large anharmonicity constants, in a previous section (Fig. 6).

A Class 6 species, the CN B-X band system, is shown in Figure 7. The one Class 7 band system, PO A-B (not shown), has the

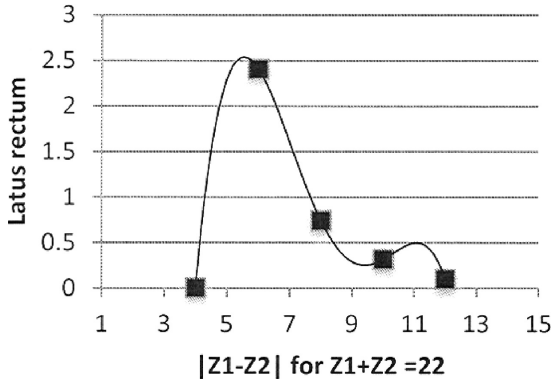

Figure 14. A plot of the latera recta for the band systems are shown in Figure 13. The trendline is a fourth-order polynomial with no basis in theory. It is characteristic of many of the band systems studied in this article that the latera recta in an isoelectronic series vary from molecule to molecule somewhat with or (as in this case) inversely to θ. A survey of the last two columns of Table 1 shows that the same is not true within classes.

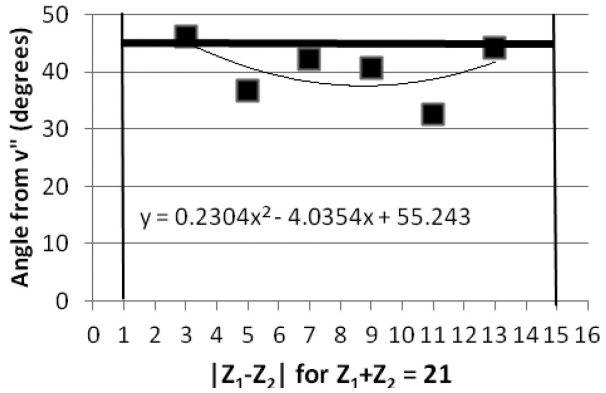

Figure 15. The $B^2\Pi_r$-$X^2\Sigma^+$ 21-electron molecule band systems. The five molecules from left to right are FMg, OAl, NSi, CP, BS, and BeCl. From left to right, the Condon loci are narrow, very wide, wide, wide, wide, and narrow in appearance. All these B states of the molecules are the second above the ground state. The vertex is at abscissa 8.401.

opposite behavior: Its Morse locus arms are outside of its SHM locus arms. Class 8 molecules are represented by Br_2, whose graphic is quite different than the preceding ones (Fig. 8).

Class 9 species are represented by an even more different graph, that of NaH A-X (Fig. 9). There is no value of $\omega_e x_e'$ for this band system in Ref. 8], so a value of 15 cm^{-1} was assigned. A value of 24 $cm^{-1}$was also assigned with little change in the graphic.

Class 10 contains plots somewhat similar to those in Class 9; it is here represented by N_2 A-X (Fig. 10) and by CO a′-X (Fig. 11).

The sketch of Herzberg on page 197,[4] Figure 12 of Nicholls,[5] and Figure 14 of Flinn et al.[7] are not identifiable as being in any of the classes described herein. We infer that the electronic states of those molecules are far from being SHM or Morse potentials.

From this limited study, it is concluded that all classes of molecules except those in Class 9 can be included in the analysis to come, and that the SHM loci appear to represent the locally maximal FCFs.

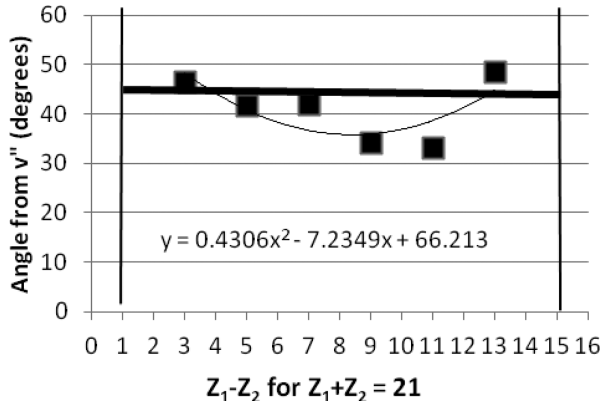

Figure 16. The $^2\Pi$-$^2\Sigma$ 21-electron molecule band systems. The five molecules from left to right are FMg, OAl, NSi, CP, BS, and BeCl. Their Condon loci are narrow, wide, narrow, wide, wide, and narrow in appearance. All the excited states of these molecules are just above the ground states. The minimum of the parabola is at $x = 8.76$.

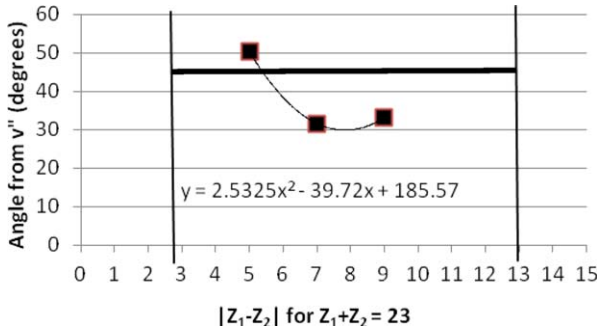

Figure 17. The angle θ for the 23 electron $^2\Pi$-$^2\Pi$ isoelectronic sequence containing the molecules SiF, PO, and SN. The Condon loci are rather narrow, with the one for PO (abscissa 7) being the most narrow. The excited states are the fifth, third, and first states above the ground state. The minimum of the parabola is at $x = 7.842$, near the center of the interval at $x = 8$. [Color figure can be viewed in the online issue, which is available at wileyonlinelibrary.com.]

Trends in Data for Fixed (C_1,C_2) Molecules

Kuz'menko and Chumak[10] give some (v',v'') = (0,0) FCFs for the isovalent molecules (C_1,C_2) = (2,7) which seem to show monotonicity. Our study of dihalide molecules would show a nice monotonic behavior for the latera recta were it not broken by F_2 and Br_2 (Fig. 12). Conversely, no monotonic behavior in the group numbers is seen when the molecules are sorted against the latera recta in Table 2. Thus, it seems that the analysis of presently collected data for homologous molecules has no promise.

Trends in Data for Isoelectronic Series of Molecules

Data

It has been shown that SHM loci represent the track of maximal $q(v',v'')$ in Deslandres tables [with the exception of LiH and NaH (Class 9)]. The sequences are shown in Table 2. The results are given in the order of decreasing electron

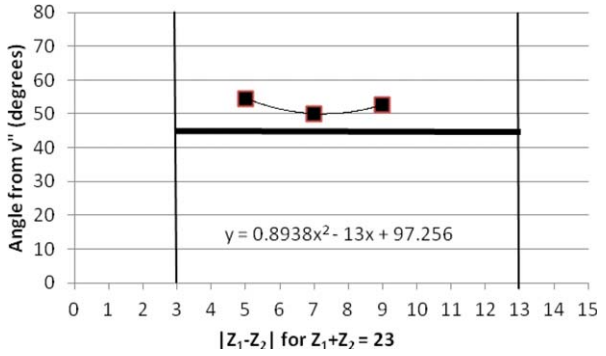

Figure 18. As same as Figure 17 except for the $^2\Sigma$-$^2\Sigma$ band systems. These band systems are unusual in that the lower electronic states are not the ground state, and indeed for PO the term labels are alphabetically reversed. The Condon loci are wide, with the least wide being for SiF. The upper and lower states for these band systems are ranked 3 and 1, 3 and 1, and 6 and 3 above the X ground states. The minimum of the parabola is at $x = 7.27$. [Color figure can be viewed in the online issue, which is available at wileyonlinelibrary.com.]

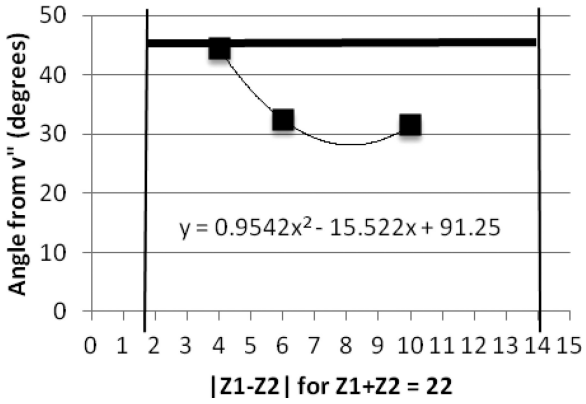

Figure 19. The angle θ for the $^3\Sigma^+$-$X^1\Sigma^+$ 22-electron sequence AlF, SiO, and SC. The excited states are the third, first, and second above the ground state, in that order. The Condon loci are narrow, wide, and narrow. The left and right boundaries are MgNe and ArBe. The vertex lies above 8.136.

populations. The molecular notations are not consistent with usual practice, so it is necessary to pay attention to which atom is first and which is second in the molecular moniker. The molecules span each sequence between two rare-gas molecules (which are shown but without data) and/or a mirror molecule. They are organized such that as Z of the left atom increases, Z of the right atom decreases, and $Z_1 - Z_2$ increases.

The figures to follow in this section show the angle θ for the SHM Condon locus of the band systems in isoelectronic sequences, given in Table 2, plotted on the difference of the atomic numbers. The data points are fitted with second degree polynomials for the only reason that the polynomials are a simple means of emphasizing the similar behavior from figure to figure; they are in terms of x, which equals $Z_1 - Z_2$. The parabolas play no role whatsoever in any of the calculations.

The heavy horizontal line is at $\theta = 45°$. In addition to the names and terms of the molecules, the captions state the qualitative appearances of the SHM loci (as used in Table 1), the relative positions of the excited states with respect to the

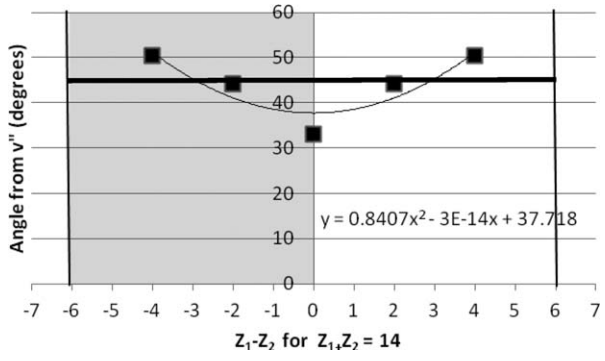

Figure 20. The angle θ of the Condon locus of the 14-electron $^1\Sigma^+$-$^1\Sigma^+$ band systems of N2, CO, and BF. The two points to the left of zero, which are OC and FB, respectively, help to draw attention to the parabolic nature of the trend line. The loci are very wide in the center, narrow at $Z_1 - Z_2 = \pm 2$ (those data points being almost at 45°) and wide at the ends. The excited states for N_2, CO, and BF are sixth, 12th, and fifth above the ground state. [Color figure can be viewed in the online issue, which is available at wileyonlinelibrary.com.]

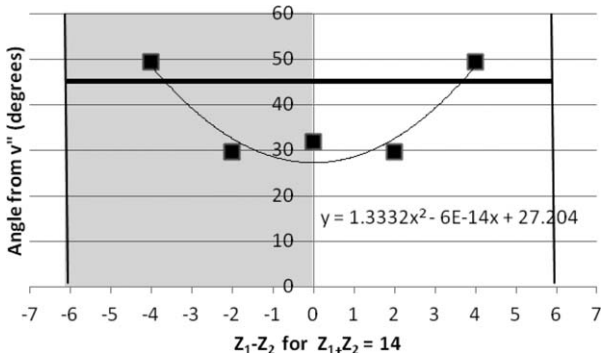

Figure 21. Same as Figure 20 but for the $^3\Sigma$-$X^1\Sigma$ band systems. The Condon loci are wide, wide, and narrow from center to end. The excited states for are the first, second, and third states above the ground state. [Color figure can be viewed in the online issue, which is available at wileyonlinelibrary.com.]

lower states, and the standard deviation of the data from a parabolic fit to the data (if there are more than three data). The exception is Figure 14, which shows how the latus rectum of the 22-electron sequence compares with the angles shown in Figure 13.

Isoelectronic series with several different molecules

Figs. 13, 14, 15, and 16.

Isoelectronic series with three different molecules

The figures in this section are similar to those preceding them except that there are only three data and Figs. 17, 18, and 19.

Isoelectronic series with a homonuclear molecule plus two heteronuclear molecules and their mirror images

The graphs presented in this section are necessarily symmetric on either side of $Z_1 - Z_2 = 0$ because the outer two data points are mirror images.

Figs. 20 and 21.

A third graphic for the $^3\Pi$-$^1\Pi$ 14-electron band systems of the same molecules appears as Figure 8.3 (with Supporting Information in Table 8.1) of Ref. [3].

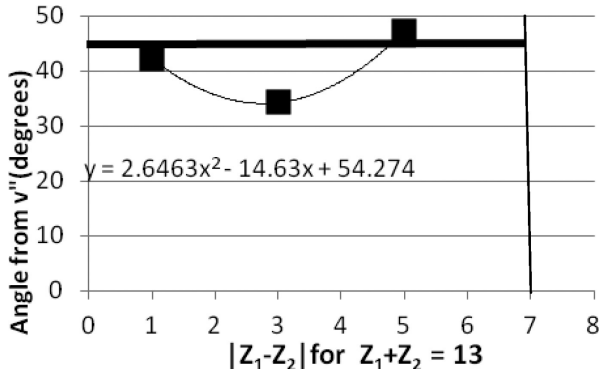

Figure 22. The $B^2\Sigma^+$-$X^2\Sigma^+$ band system of NC, OB, and FBe. Why the trend line rises at the left remains to be investigated; the important thing is that the data at right rise as they approach NeLi. The qualitative appearances of the loci are wide, wide, and narrow, respectively; the excited states are all second in order above the ground state.

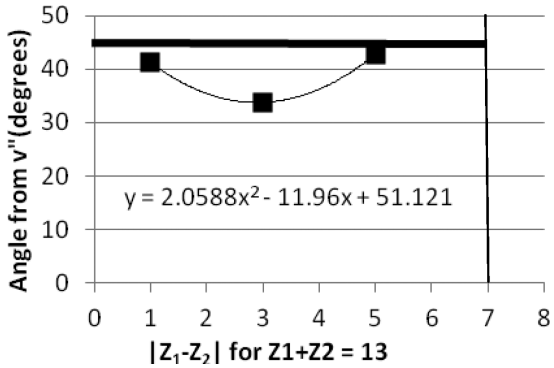

Figure 23. As same as Figure 23 except that the period number of the first atom changes progressively (OB and FBe changed to SB and BrBe). This graph was made as a computer experiment to find out whether a homologous-isoelectronic sequence would resemble pure isoelectronic sequences (this one does). The loci for NC, SB, and BrBe are wide, very wide, and narrow; the upper states are all immediately above the ground state.

Isoelectronic series with no homonuclear molecule, having three heteronuclear molecules and their mirror images

The graphs in this section are symmetric on either side of $Z_1 - Z_2 = 0$ because there are mirror image data (not shown) at negative abscissae. One would expect the data have a minimum at $Z_1 - Z_2 = 0$. Why they rise as they approach $|Z_1 - Z_2| = 0$ (which is not a rare-gas, or in fact any, molecule) is unknown.

Figs. 22, 23, and 24.

The Upper and Lower State Vibration Frequencies

The periodicity just demonstrated in the section Trends in Data For Isoelectronic Series of Molecules is of θ, the tangent of which is the ratio, by eq. (1), of the upper to the lower vibration frequencies. These two vibration frequencies are plotted in Figures 25 and 26. The ratios of the ordinates in these two figures are related to the tangents of the angles θ in Figures 13 and 16 in the following manner: First, we note that if $\omega_e' = \omega_e''$ at any $|Z_1 - Z_2|$, then θ will be 45° in Figures 13 and 16, and the data points will lie together in Figures 25 and 26. Then for all the data, we calculate the actual differences $\theta - 45°$ and $\omega_e' - \omega_e''$ and normalize them to percentages by division with 45° and ω_e''. These steps are shown in Table 3.

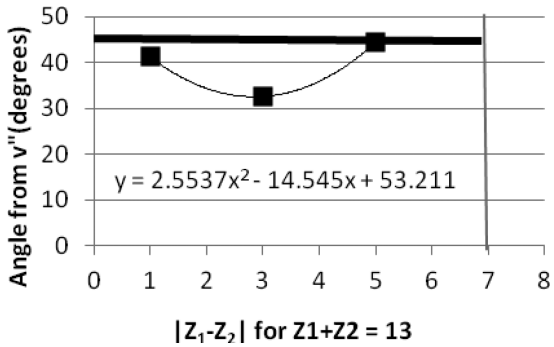

Figure 24. As same as Figure22 except that the term symbols are now $^2\Pi^+$-$^2\Sigma^+$. The excited states are immediately above the ground state.

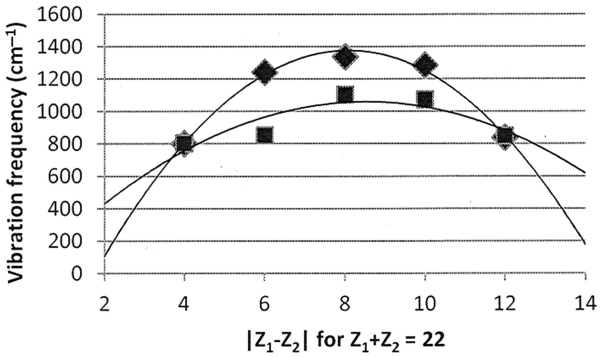

Figure 25. The upper and lower series are the upper and lower state vibration frequencies ω_e' and ω_e'' for the AlF, SiO, PN, SC, and ClB 22-electron $^1\Pi_i$-$^1\Sigma^+$ band systems. The ω_e' data are very close to the $\omega e''$ data at abscissae 4 and 12 and are less in between, which causes the data points in Figure 13 to drop down below 4 and 12.

Discussion

The first result of this investigation is the clarification that Yes, molecules do echo atomic periodicity—data plots for θ rise as the series of molecules approach one with a magic-number atom—and No, they do not echo atomic periodicity in detail, that is, in the data profiles between molecules with magic-number atoms.

The second result of this investigation is to place molecular periodicity on a more quantum footing than it was with evidence based on previous graphical studies. This has been accomplished by study of band-system Deslandres tables of FCFs. The study has found that the force constants of upper states become greater, compared to those of the lower states, as diatomics in any series approach a rare-gas molecule (very likely the extreme cases, cf. the reduced potential curves of Jenč[11,12]).

There is a parallel approach based on computed ground-state molecular configurations for homonuclear and hydride molecules (pp. 341 and 344 of Ref. 4]). If a complete set of upper and ground state configurations for even just main-group diatomics were available, this approach toward

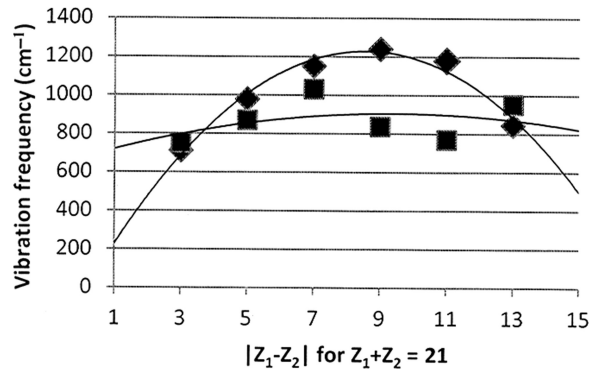

Figure 26. **As** same as Figure 25 but for the FMg, OAl, NSi, CP, BS, and BeCl $^2\Pi$-$^2\Sigma$ band systems (Fig. 16). As in Figure 25, the locations of the ω_e' data with respect to the ω_e'' data correspond to the deviation of θ from the trend line (in Fig. 16).

Table 3. Molecules, atomic number differences, and the Condon locus symmetry angle θ, all taken from Table 2. Then, how far the data points fall below the 45° heavy lines of Figures 13 and 16 in columns three to five; and how far the upper state vibration frequencies fall below the lower state vibration frequencies in Figures 25 and 26 in columns six and seven. The upper entries pertain to the 22-electron $A^1\Pi_i$-$X^1\Sigma^+$ sequence of Figures 13 and 25; the lower entries pertain to the 21-electron $B^2\Sigma^+$-$X^2\Sigma^+$ sequence of Figures 16 and 26. Data have been rounded to two significant figures, with the third shown in parentheses where needed. The correlation coefficient compares the two columns enclosed in boxes.

Species	Z_1-Z_2	θ (°)	$\theta-45$ (°)	% of 45	ω_e'-ω_e''	% of ω_e''
AlF	4	45.06	0.06	0.13	1.68	0.21
SiO	6	34.48	−10.52	−23.38	−388.8	−45.59
PN	8	39.52	−5.48	−12.18	−234.2	−21.23
SC	10	39.87	−5.13	−11.40	−211.7	−19.72
ClB	12	45.34	0.34	0.76	9.92	1.17
		Coefficient of correlation			0.99(7)	
FMg	3	46.54	1.54	0.22	39.25	0.04(4)
OAl	5	41.62	−3.38	−0.35	−109.18	−0.05(0)
NSi	7	41.84	−3.16	−0.27	−120.33	−0.04(2)
CP	9	34.00	−11.00	−0.89	−403.35	−0.13
BS	11	33.12	−11.88	−1.01	−410.17	−0.16
BeCl	13	48.37	3.37	−0.40	105.8	0.08(2)
		Coefficient of correlation			0.99(8)	

explaining the periodicity of diatomic molecules could be very persuasive.

Palma's group in Mexico City[13–15] has investigated FCFs for arbitrary electronic potentials, but does not appear to have computed Condon loci for the factors.

This investigation began as a yet another search for periodicity in properties of molecules[1,3].Others have participated in the search.[16] Kibler, of l'Université Claude Bernard Lyon I, has shown how group theory undergirds atomic and fundamental-particle periodicity[17,18] and how q-deformed groups reproduce the shell structures of neutral atoms, of positive ions, and of hydrogen-like ions depending on the value of q.[19]

Acknowledgments

Brian Clark made Figures 3 through 11 while an undergraduate research assistant at SAU.

Keywords: periodicity • molecules • Franck · Condon factors • Condonloci•forceconstants

How to cite this article: R. Hefferlin, J. Sackett, J. Tatum, *Int. J. Comput. Chem.* **2013**, *113,* 2078–2089. DOI: 10.1002/qua.24469

[1] R. Hefferlin, Periodic Systems of Molecules and Their Relation to the Systematic Analysis of Molecular Data, Chapter 5; Edwin Mellin Press: Lewiston, New York, **1989**. Plates 1–6 and 8.
[2] F. -A. Kong, W. -Q. Wu, *Sci. China Chem.* **2012**, *55*, 618.
[3] R. Hefferlin, J. Sackett, J. Tatum, Progress in Theoretical Chemistry and Physics, Vol. *26*; K. Nishikawa, J. Maruani, Eds.; In Proceedings of the Conference on Quantum Systems in Chemical Physics XVI, Kanazawa, Japan, 2011; Springer: London, **2012**.
[4] G. Herzberg, Molecular Spectra and Molecular Structure, Vol. *I*: Spectra of Diatomic Molecules; Krieger Publishing Company: Van Nostrand, New York, **1950**.
[5] R. W. Nicholls, *J. Quant. Spectrosc. Radiat. Transfer* **1982**, *28*, 481.
[6] J. M. Standard, B. K. Clark, *J. Chem. Educ* **1999**, *76*, 1363.
[7] D. J. Flinn, R. J. Spindler, S. Fifer, M. Kelly, *J. Quant. Spectrosc. Radiat. Transfer* **1964**, *4*, 271.
[8] K. P. Huber, G. Herzberg, Constants of Diatomic Molecules; Van Nostrand Reinhold: New York, **1979**.
[9] B. Karthikeyan, Studies on Molecular Species Identified in Solar and Allied Spectra by Spectroscopic Techniques (dissertation); Madurai Kamaraj University: Madurai, India, **2007**.
[10] N. E. Kuz'menko, L. V. Chumak, *J. Quant. Spectrosc. Radiat. Transfer* **1986**, *35*, 419.
[11] F. J. Jenč, *Mol Spectrosc* **1967**, *24*, 284.
[12] F. J. Jenč, *Spectrochim Acta* **1967**, *24A*, 259.
[13] F. J. Medénlez, L. Sandoval, A. Palma, *J. Mol. Struct. (THEOCHEM)* **2002**, *580*, 91.
[14] A. Palma, L. Sandoval, K. Churyumov, V. Chavushyan, A. Berezhnoy, *Int. J. Quantum Chem*. **2007**, *107*, 2650.
[15] L. Sandoval, I. Urdeneta, A. Palma, *Far East J. Math. Sci*. **2012**, *60*, 1.
[16] R. Hefferlin, In Philosophy of Chemistry; D. Baird, E. Scerri, L. McIntyre, Eds.; Springer: Dordrecht, **2006**; pp. 221–243.
[17] M. Kibler, On a Group-Theoretical; Technical University: Prague, 2004 (arXiv:-quant-ph/0409209). See also: M. R. Kibler, *Mol. Phys*. **2004**, *102*, 1221.
[18] M. R. Kibler, In The Periodic Table: Into the 21st Century, Chapter 11; D. H. Rouvray, R. B. King, Eds.; Research Studies Press: Baldock, Hertfordshire, England, **2004**.
[19] T. Négadi, M. Kibler, *J. Phys. A* **1992**, *25*, L157.

Received: 7 January 2013
Revised: 28 March 2013
Accepted: 3 April 2013
Published online on 30 May 2013